



Published in final edited form as:

Circ Cardiovasc Genet. 2014 August ; 7(4): 434–443. doi:10.1161/CIRCGENETICS.113.000448.

Sarcomere Mutation-Specific Expression Patterns in Human Hypertrophic Cardiomyopathy

Adam S. Helms, MD^{1,*}, Frank Davis, BS^{1,*}, David Coleman, BS¹, Sarah Bartolone, BS¹, Amelia A. Glazier, BS², Francis Pagani, MD, PhD³, Jaime M. Yob, MS¹, Sakthivel Sadayappan, PhD⁴, Ellen Pedersen, BS⁵, Robert Lyons, PhD⁵, Margaret V. Westfall, PhD^{2,3}, Richard Jones, PhD⁶, Mark W. Russell, MD⁷, and Sharlene M. Day, MD¹

¹Department of Internal Medicine, University of Michigan, Ann Arbor, MI

²Department of Molecular and Integrative Physiology, University of Michigan, Ann Arbor, MI

³Department of Cardiac Surgery, University of Michigan, Ann Arbor, MI

⁴Department of Cell and Molecular Physiology, Health Sciences Division, Loyola University Chicago, Maywood, IL

⁵Department of Sequencing Core, University of Michigan, Ann Arbor, MI

⁶MS Bioworks, Ann Arbor, MI

⁷Department of Pediatrics, University of Michigan, Ann Arbor, MI

Abstract

Background—Heterozygous mutations in sarcomere genes in hypertrophic cardiomyopathy (HCM) are proposed to exert their effect through gain-of-function for missense mutations or loss-of-function for truncating mutations. However, allelic expression from individual mutations has not been sufficiently characterized to support this exclusive distinction in human HCM.

Methods and Results—Sarcomere transcript and protein levels were analyzed in septal myectomy and transplant specimens from 46 genotyped HCM patients with or without sarcomere gene mutations and 10 control hearts. For truncating mutations in *MYBPC3*, the average ratio of mutant:wild-type transcripts was ~1:5, in contrast to ~1:1 for all sarcomere missense mutations, confirming that nonsense transcripts are uniquely unstable. However, total *MYBPC3* mRNA was significantly increased by ~9 fold in HCM samples with *MYBPC3* mutations compared to control hearts and to HCM samples without sarcomere gene mutations. Full-length MYBPC3 protein content was not different between *MYBPC3* mutant HCM and control samples and no truncated proteins were detected. By absolute quantification of abundance (AQUA) with multiple reaction monitoring, stoichiometric ratios of mutant sarcomere proteins relative to wild-type were strikingly variable in a mutation-specific manner, with the fraction of mutant protein ranging from 30–84%.

Correspondence: Sharlene M. Day, 1150 W. Medical Center Drive, 7301 MSRB III, Ann Arbor, MI 48109, Tel: (734) 615-7917, Fax: (734) 936-8266, sday@umich.edu.

*contributed equally

Disclosures: None

Conclusions—These results challenge the concept that haploinsufficiency is a unifying mechanism for HCM caused by *MYBPC3* truncating mutations. The range of allelic imbalance for several missense sarcomere mutations suggests that certain mutant proteins may be more or less stable, or incorporate more or less efficiently into the sarcomere than wild-type proteins. These mutation-specific properties may distinctly influence disease phenotypes.

Keywords

hypertrophic cardiomyopathy; sarcomere; gene expression; human; proteomics; expression/regulation

Introduction

The most common Mendelian cardiovascular condition, hypertrophic cardiomyopathy (HCM), is defined by unexplained cardiac hypertrophy and can be complicated by left ventricular outflow tract obstruction, atrial and ventricular arrhythmias, sudden cardiac death, and heart failure.¹ Sarcomere gene mutations account for ~50–75% of the genetic basis of HCM, the majority found in the two largest genes, *MYBPC3* (myosin binding protein C) and *MYH7* (β -myosin heavy chain).² Despite identification of >1,000 sarcomere gene mutations, molecular mechanisms that elicit disease phenotypes are incompletely defined.³ One fundamental question pertains to the nature of the gene product derived from the mutant allele. Most sarcomere mutations result in a single amino acid substitution that encodes a full-length protein. The exception is *MYBPC3* where >50% of mutations create a premature-termination codon (PTC).⁴ The widely accepted hypothesis is that truncating *MYBPC3* mutations cause haploinsufficiency, as opposed to missense mutations which incorporate into the sarcomere and act in a dominant-negative fashion.³ Previous studies in human HCM addressing this hypothesis have been constrained by small numbers of samples with unique mutations. Here, we comprehensively analyze sarcomere gene and protein levels from a large number of cardiac specimens from HCM patients of known genotype. We hypothesized that allelic balance between wild-type and mutant sarcomere proteins is variable and mutation-specific, reflecting differential stability or efficiency of sarcomere incorporation compared to the wild-type protein. We further proposed that haploinsufficiency may not be the primary driver of disease progression in HCM associated with *MYBPC3* truncating mutations.

Methods

An expanded methods section is available in the on-line only Data Supplement.

Human heart tissue procurement

Ventricular myocardial tissue was snap frozen in liquid N₂ or placed in formalin at the time of collection. This study had the approval of the University of Michigan Institutional Review Board (IRB) and subjects gave informed consent.

Transcript analysis

RT-PCR, cDNA sequencing, and RT-qPCR were performed by standard techniques (see on-line data supplement). An RT-qPCR assay was used to determine allelic specific expression in the samples containing splice-site mutations, while the single-base extension method was used in samples containing single nucleotide variants that resulted in premature stop codons (see on-line supplemental methods and Supplementary Table 1).

Protein preparation, quantification and immunolocalization

Immunoblotting, immunofluorescent imaging, myofilament fractionation, and extraction of insoluble proteins were performed by established methods (see on-line data supplement).

Absolute Quantification of Abundance (AQUA)

Myofilament proteins were separated using SDS-PAGE and Coomassie stained. The protein of interest was gel excised. After in-gel enzymatic digestion, samples were analyzed by nano LC/MS/MS performed in the Orbitrap at 70,000 FWHM and 17,500 FWHM resolution, respectively. In some cases, peptides were post-translationally modified (ex. Met oxidation) or contained missed cleavages. The abundance of mutant and wild type sarcomere proteins within each sample was then determined using isotopically-labeled synthetic AQUA peptides corresponding to each form of wild-type and mutant peptides for each individual sample. Samples were analyzed by LC-SRM/MS with a Waters NanoAcquity HPLC system interfaced to a ThermoFisher TSQ Quantum Ultra. Peak areas for the wild-type or mutant endogenous peptide were expressed as a ratio to their corresponding AQUA peptides allowing the mole ratio of wild type versus mutant peptide to be calculated. Molar amounts from all wild-type and mutant peptides were summed, and expressed as a percentage of total protein. More details can be found in the on-line data supplement.

Statistical analysis

All values are expressed as mean \pm SEM unless otherwise indicated. Normality was determined by the Shapiro-Wilk test. Western blot data for TNNT2, ACTC1, TNNT3 and MYL2 were normally distributed and analyzed by 1 way ANOVA. For non-normally distributed data, analyses were performed on ranks using the Mann Whitney rank sum test for 2 group comparisons (PTC vs. non-PTC containing transcripts) or the Kruskal Wallis test for multiple group comparisons. Race and gender comparisons among patient groups were analyzed by chi-square. All statistical analyses were performed using Sigma Stat 12.5 or IBM® SPSS® Statistics with a two-sided P value <0.05 indicating significant differences.

Results

Demographics, clinical characteristics, and genetics

We utilized heart tissue from 10 non-failing donor hearts and 46 HCM patients of known genotype: 42 from myectomy samples, 1 at the time of left ventricular assist device [c. 1928-2 A>G (a)], and 3 at the time of transplant [MYBPC3 Trp890*(a), MYH7 Thr1377Met, MYH7 Gly708Ala]. Control and HCM patients were comparable in age and gender (Table 1). Racial background was white, except for 2 control hearts from black

donors. Ethnicity was hispanic for 2 hearts (1 control and 1 HCM) and Middle Eastern for 1 heart (HCM). Wall thickness was greater in all HCM groups compared to controls ($P < 0.05$), and ejection fraction was higher in HCM groups with sarcomere gene mutations compared to controls ($P < 0.05$). Neither wall thickness nor ejection fraction differed among HCM groups differentiated by genotype. Most mutations in *MYBPC3* were truncating mutations, while those in other genes were missense (Supplementary Table 2). The same mutation was present in 2 samples in 7 instances (6/7 were unrelated, 1/7 from siblings [*MYBPC3* c.3330+2 T>G]), designated in the figures and text as (a) and (b) respectively.

cDNA sequencing of *MYBPC3* splice site mutations confirm presence of PTCs

We sequenced cDNA from all myocardial samples containing known or putative splice site mutations in *MYBPC3*. All mutations located in a consensus splice donor or acceptor site created a PTC in the mutant transcript (Supplementary Table 3). All mutations in exon or intron splice donor sites ($n=5$) resulted in skipping of the exon containing, or preceding, the mutation (except c.2308 G>A for which a mutant transcript was not detectable), while mutations in intron splice acceptor sites ($n=2$) resulted in inclusion of the intron containing the mutation (Supplementary Figure 1).

Sarcomere gene mutations confer variable allele-specific expression

For truncating mutations, the mutant transcripts constituted a minority of total transcripts (range undetectable to 44%) for both the *MYBPC3* splice site mutations as determined by RT-qPCR (Figure 1A, left panel), and for the non-splice site *MYBPC3* truncating mutations (Figure 1A, right panel) as determined by single-base extension. These data are consistent with the hypothesis that truncating mutant transcripts with PTCs are susceptible to degradation by nonsense-mediated RNA decay (NMD).^{5, 6}

Mutations in exon splice sites could yield both missense and nonsense transcripts, depending on the extent to which the mutation alters splicing.⁷ Therefore, missense transcripts were analyzed using the single base extension reaction in samples with exon splice site mutations. A missense transcript for c.1624G>C (Glu542Gln) was present, in addition to the mutant splice variant transcript, and constituted 13 and 16% of total full-length *MYBPC3* transcripts for each sample respectively (Figure 1B). However, no missense transcript was detected for either c.772G>A (Glu258Lys) sample, indicating that 100% of the transcripts from the mutant allele exist as truncating mutant transcripts. The Sequenom software was not able to design primers for the *MYBPC3* mutation c.2308G>A (Asp770Asn). However, amplification of cDNA using primers in exons 22 and 24 yielded a single band containing only wild-type sequence (Supplemental Figure 1C). No band corresponding to the mutant transcript was detectable with use of a forward primer that spanned the junction of exon 22–24, suggesting that this particular mutation efficiently alters splicing (likely resulting in skipping of exon 23), but that the mutant PTC-containing transcript is undetectable due to instability. Less likely is the possibility that splicing is altered at a distant splice site not detected using these primers.

The ratio of mutant to wild-type transcript for *MYBPC3* c.3742_3759dup (Gly1248_Cys1253dup) could not be precisely quantified because the wild-type transcript

could not be uniquely amplified (addition of “A” after extension primer could be either wild-type or second repeat of mutant transcript). However, the mutant transcript was identified in a standard sequencing reaction (Supplementary Figure 2A) and constituted at least 30% of the total by single base extension (i.e. 30% of the extension product contained the first nucleotide of the duplicated sequence).

Using single base extension, ratios of all true missense mutations in *MYBPC3*, *MYH7*, *MYL2* and *TNNT2* were present at the expected ~1:1 ratio with wild-type transcripts (Figure 1B). The Sequenom software could not design primers for *TPM1* c.850A>G (Ile284Val), perhaps because it is in the terminal codon. However, cDNA sequencing showed polymorphism at that site (Supplementary Figure 2B).

Overall, PTC-containing transcripts in *MYBPC3* are significantly less abundant than transcripts from non-PTC-containing mutant alleles from either *MYBPC3* or other sarcomere genes (mean $16 \pm 3\%$ vs. $47 \pm 1\%$ of the total respectively, $P < 0.00001$), consistent with their recognized targeting for NMD. However, the degree of susceptibility to NMD appears to be highly variable given the wide range observed for the relative proportion of *MYBPC3* truncating mutant transcripts.

Increased total *MYBPC3* mRNA abundance in samples containing *MYBPC3* mutations

To determine effects of mutant transcript instability on total *MYBPC3* transcript abundance we performed RT-qPCR in samples from 4 groups: control donor hearts (n=7), HCM hearts from patients without sarcomere gene mutations (n=7), HCM hearts with *MYBPC3* mutations (n=18), and HCM hearts with *MYH7* mutations (n=6). Unexpectedly, mean total *MYBPC3* transcript levels were increased in the *MYBPC3* mutation group compared to non-failing donor hearts ($p=0.02$) and HCM without sarcomere mutations ($p=0.003$, Figure 1C, left panel). Increased *MYBPC3* expression was consistent across all samples, with at least a 2-fold increase in total transcript level in each individual sample, including the 2 samples with missense mutations (Arg495Gln). This contrasts with *MYH7* abundance for which no differences were observed among the groups (Figure 1C, right panel). The magnitude of increased *MYBPC3* expression did not appear to correlate with the domain location of the mutation. *MYBPC3* expression was highly variable in the samples with *MYH7* mutations, but with no significant difference in the mean transcript level compared to controls or sarcomere negative HCM. These results were also supported by simple RT-PCR analysis of representative samples with a separate pair of PCR primers (Figure 1D). These results suggested that transcriptional upregulation of *MYBPC3* compensates for degradation of the mutant transcript.

Comparable *MYBPC3* protein levels between HCM samples with *MYBPC3* mutations and control hearts

To determine if transcriptional upregulation of *MYBPC3* in samples containing *MYBPC3* mutations prevented haploinsufficiency at the protein level, full length *MYBPC3* protein was detected by immunoblotting using an antibody targeting the N-terminus. None of the HCM groups (*MYBPC3* mutations, non-*MYBPC3* mutations, no sarcomere mutation) demonstrated a significant difference in *MYBPC3* protein abundance compared to control

hearts (Figure 2A and B). However, among the HCM groups, samples with mutations in genes other than *MYBPC3*, or without sarcomere gene mutations, had a significantly greater abundance of MYBPC3 protein in comparison to samples with *MYBPC3* mutations ($P < 0.001$). Other sarcomere proteins were similar in abundance among different HCM groups and controls (Supplementary Figure 3A). MYBPC3 protein levels were not significantly different between control heart samples and samples obtained from failing hearts due to non-ischemic or ischemic cardiomyopathies ($n = 14$, Supplementary Figure 3B), suggesting that advanced heart failure itself does not alter MYBPC3 abundance.

The presence of a *MYBPC3* mutation did not appear to cause MYBPC3 mislocalization since cell fractionation experiments showed MYBPC3 to be present only in the myofilament fraction, and immunofluorescence imaging showed only normal localization of the protein in the sarcomere A-band (Figure 3A and B). Consistent with previous reports,^{8,9} no truncated MYBPC3 proteins were detected by immunoblot. We also analyzed several samples by LC/MS/MS of a trypsin digest of a myofilament fraction in solution or gel-extracted fragments at the expected truncated molecular mass with and without extraction of insoluble proteins, but did not detect peptides containing the corresponding mutation (data not shown).

Given the variability in mutant transcript stability, we considered the possibility of translation re-initiation that could stabilize truncating mutant transcripts. We probed samples containing truncating *MYBPC3* mutations with an antibody raised against the C-terminal domain of MYBPC3. However, there were no unique bands containing MYBPC3 peptides detectable by LC/MS/MS (data not shown).

Stoichiometry of mutant and wild-type sarcomere missense proteins is highly heterogeneous in human HCM

The respective sarcomere protein levels of heterozygous wild-type and mutant alleles are presumed to be present in equimolar quantities in HCM, but limited data are available in human hearts. Here, we used absolute quantification of abundance (AQUA), a highly sensitive and quantitative approach to determine the stoichiometric ratios of wild-type to missense sarcomere mutant proteins (Figure 4A). Raw data are presented in Supplementary Table 4. For 5 samples with different *MYH7* mutations and one with the TPM1 Ile284Val mutation, the ratio of wild-type to mutant protein was at or near the expected 1:1 ratio (Figure 4B). However, in the case of the sample with the Ile323Asn mutation in *MYH7*, the mutant peptide was >2 fold more abundant than the wild-type peptide. The opposite was true for the sample with the Gly708Ala mutation in *MYH7*, where the mutant peptide constituted only 10% of total *MYH7* peptide (RT-PCR analysis of this sample confirmed normal splicing, Supplementary Figure 1D). For *MYL2*, the mutant peptides containing Arg161 constituted only 31% of the total (Figure 4B). The opposite was true for the TNNT2 mutation, where the mutant peptide containing Ala86 represented 84% of the total TNNT2 peptide. Similarly, in both samples from unrelated patients carrying the Arg495Gln mutation in *MYBPC3*, the mutant peptide was predominantly expressed over wild-type, 62–69% of total MYBPC3. In two hearts from patients undergoing cardiac transplantation (*MYH7* Thr1377Met and Gly708Ala), relative expression of mutant to wild-type *MYH7* peptides

did not display significant regional variation. Collectively, these results suggest differences in intrinsic stability or sarcomere incorporation efficiency for a substantial subset of missense proteins compared to their wild-type counterparts.

Little or no detectable full length mutant protein was detected for *MYBPC3* mutations in exon splice sites or for a C-terminal in frame duplication. In 2 samples from unrelated patients with an exon splice site mutation in *MYBPC3*, Glu542Gln, only 2–5% of the full-length protein was derived from the mutant allele. As expected based on the absence of missense mutant transcripts for samples containing *MYBPC3* Glu258Lys and Asp770Asn mutations, only wild-type peptides were detected. Finally, in the sample containing *MYBPC3* Gly1248_Cys1253dup, the duplicated peptide was also not detected despite detection of mutant transcript, implying that the C-terminal duplication destabilizes the protein.

Together, these data demonstrate allelic imbalance for a large number of HCM sarcomere missense mutations across different genes. Since single base extension reactions uniformly showed comparable quantities of mutant and wild-type mRNA for samples with missense mutations, the basis for this allelic variation at the protein level would appear to be translational or post-translational. Interestingly, the degree of allelic imbalance (quantified by the absolute deviation of the mutant to wild-type allelic ratio from the predicted 1:1) significantly correlated with younger age at surgery and younger age at diagnosis ($p < 0.01$, Figure 4C).

Discussion

We present a comprehensive analysis of mutant sarcomere gene expression, protein abundance, and stoichiometry from human HCM heart tissue. A major finding from this study is an unexpected and paradoxical 9-fold up-regulation of total *MYBPC3* mRNA in samples containing *MYBPC3* truncating mutations, which we presume to be compensating for instability of the mutant transcript to maintain normal levels of full-length *MYBPC3* protein. This discovery counters the prevailing notion that *MYBPC3*-mutation HCM is driven by haploinsufficiency. In addition, using a highly quantitative proteomic approach, we have shown that many samples containing missense mutations in *MYBPC3* and other sarcomere genes display a marked deviation from the expected 1:1 ratio of mutant to wild-type protein, despite comparable transcript levels. This finding suggests variable sarcomere incorporation and/or instability of mutant sarcomere proteins.

Variability in altered splicing for different *MYBPC3* splice site mutations

A substantial proportion of mutations in *MYBPC3* are located in splice site junctions. Correct predictions of whether and to what degree these mutations alter splicing has critical implications for disease mechanisms elicited by these mutations. Splice predictions by in silico models, in vitro splice reactions,¹⁰ or sequencing of peripheral blood leukocyte mRNA^{4, 11} may not accurately predict the consequences of a splice site mutation in the relevant tissue.¹² In this study, we confirmed altered splicing and generation of a PTC from myocardium of all HCM patients harboring *MYBPC3* mutations in consensus splice sites. The same mutation present in different samples consistently produced the same splice

defect, implying that the manner in which splicing is altered is inherent to a particular mutation. For all splice donor mutations, we confirmed previous predictions of exon skipping.⁴ However, both splice acceptor mutations demonstrated intron inclusion as opposed to exon skipping.^{10, 11} For the exon splice site mutation Glu542Gln, we demonstrated not only a splice-defective transcript, but also a full-length missense transcript that was not previously appreciated.¹³ Confirmation of the splice products for each mutation also prevented misclassification of mutations in exon splice sites as missense,^{8, 14, 15} with important implications for disease pathogenesis.

MYBPC3 transcript analysis supports variable efficiency of nonsense-mediated RNA decay for truncating mutant transcripts

Disease mechanisms may also be influenced in part by the relative instability of PTC-containing *MYBPC3* mutant transcripts. In relation to wild-type transcripts, PTC-containing mutant *MYBPC3* transcripts were markedly lower in abundance compared to non-PTC transcripts, consistent with previous reports^{8, 9} but with notable differences. First, the mean fraction of mutant transcripts was lower than in previous studies (16% vs 25–33%), and with considerably greater patient to patient variability (0–44% of the total), implying differential mutation-specific susceptibility to NMD. For most mutations, similar levels of truncating transcripts were observed for the same mutation studied in 2 unrelated HCM patient samples, suggesting that NMD efficiency is primarily intrinsic to a particular mutation. All PTCs were located more than 55 nucleotides upstream of the last intron and therefore all mutant transcripts would be expected to be targets for NMD.^{16, 17} Despite the tendency for PTCs situated more 5' to elicit NMD more efficiently than those downstream,¹⁷ there was no obvious association between PTC location and abundance of the mutant transcript. Translation re-initiation can rescue a mutant transcript from NMD as observed in β -thalassemia¹⁸ and long QT syndrome.¹⁹ However, we could not identify any stable MYBPC C-terminal peptides that would implicate this mechanism as an explanation for the variability in mutant transcript stability.

Regardless of the mechanism, variable NMD efficiency has important consequences for disease pathogenesis and potential therapies. NMD can be beneficial in conditions where the mutant protein is toxic²⁰ or has a dominant-negative effect,²¹ but detrimental when the mutant protein retains partial functionality.^{22–24} The role of NMD and mechanisms underlying variable susceptibility of individual *MYBPC3* mutant transcripts will also be key determinants of the efficacy of future targeted therapeutics for HCM, such as PTC read-through strategies.⁶

Evidence for compensatory upregulation of MYBPC3 challenges haploinsufficiency disease model

Complete absence of the full-length MYBPC3 protein is clearly sufficient to cause severe dilated cardiomyopathy both in mice and in humans.^{25–27} However, these observations do not necessarily implicate loss of functional protein as the primary mechanism underlying the heterozygous condition in HCM. While total *MYBPC3* transcript abundance has not been previously assessed in human HCM samples, only a modest reduction in total MYBPC3 protein (~25–30%)^{8, 9, 28} or even an increase¹⁵, has been observed in *MYBPC3* mutant

samples compared to control hearts, reflecting at least a partial compensatory increase in wild-type protein expression. A similar modest reduction in total protein is observed in heterozygous *MYBPC3* knock-out or knock-in mouse models, ~10–25%.^{7, 25, 29} In the present study comprising a larger number of HCM samples with unique mutations and control samples than in previous reports, MYBPC3 protein levels were no different in human HCM samples with *MYBPC3* truncating mutations compared to control hearts. These data strongly challenge the hypothesis that haploinsufficiency of MYBPC3 is the primary mechanism of disease.

As an alternate hypothesis to haploinsufficiency, we suggest that the primary mechanism driving disease progression in *MYBPC3*-mutation HCM may be related to the burden of truncated mutant proteins. Even though the relative abundance of mutant transcripts is limited by NMD, the marked increase in total MYBPC mRNA predicts excess production of protein from both alleles. Two specific mechanisms are supported by previous investigations. First, truncated proteins are inherently misfolded and may induce cytotoxicity by overwhelming protein quality control systems. Truncated proteins derived from *MYBPC3* truncating mutations are substrates for the proteasome, cause proteasome dysfunction and form cytosolic aggregates.^{7, 30, 31} Proteasome impairment is also evident in human HCM hearts, and is more pronounced in patients with sarcomere gene mutations.³² A second possible mechanism supported by experimental models is that truncated MYBPC3 may incorporate into the sarcomere inefficiently, causing disruption of myofibrillar architecture, functional cardiac impairment, heart failure and increased mortality.^{33–35} The inability to identify truncated proteins in hearts with *MYBPC3* mutations does not exclude these possibilities as low level or transient expression of truncated peptides could escape detection by available methods. Marked alterations in protein structure and folding could reduce binding affinity of mutant proteins for available MYBPC3 antibodies, even those recognizing N-terminal epitopes.

It is certainly possible that haploinsufficiency of MYBPC3 drives early cellular remodeling with other mechanisms manifesting once full-length protein levels are restored. This mechanistic transition has been previously reported in mice with a frameshift lamin A (*LMNA*) mutation, in which early remodeling was attributed to haploinsufficiency, while later disease progression occurred despite normalization of LMNA levels and was associated with accumulation of toxic aggregates and proteasome impairment.³⁶ Since our analyses utilize human samples with a mature form of the disease, we cannot rule out haploinsufficiency early in the disease course. It is also important to recognize that although MYBPC3 protein levels were the same in *MYBPC3* mutant HCM samples as in control hearts, they were lower compared to HCM samples harboring other mutations or without sarcomere mutations. The significance of this finding is unclear at this time but merits further consideration. We would contend that haploinsufficiency and dominant negative effects of mutant proteins are not mutually exclusive and it is unlikely that a single mechanism can explain how different truncating mutations in *MYBPC3* trigger disease onset and drive progressive remodeling over a human lifespan.

The marked increase in *MYBPC3* mRNA abundance in *MYBPC3* mutant samples compared to control hearts and HCM samples without sarcomere mutations in the present study may

be driving the compensatory response at the protein level to maintain stoichiometry between full-length MYBPC3 and other myofilament proteins. Since the mechanisms that regulate *MYBPC3* transcription, translation and protein turnover are largely unknown, it is difficult to speculate on the precise signals through which such a response may be occurring. However, it is possible that instability of mutant transcripts and/or proteins may be somehow involved. The discrepancy in the magnitude of increase in transcript to protein abundance can probably be explained by the tight regulation of sarcomere stoichiometry which precludes a significant over-abundance of any one component.^{37, 38} For example, in a transgenic mouse model expressing a mutant MYBPC3 truncated peptide, the mRNA level is 5-fold increased without any difference in MYBPC3 protein stoichiometry.³⁴

An increase in *MYBPC3* transcript abundance was not limited to samples harboring *MYBPC3* truncating mutations, but was also evident in 2 samples with *MYBPC3* missense mutations and in myectomy samples with *MYH7* mutations (2 transplanted hearts had decreased expression). This upregulation, unique to sarcomere HCM, reveals the complexity of *MYBPC3* gene regulatory pathways in human HCM and warrants further exploration in model systems.

Allelic balance for missense sarcomere mutations is post-transcriptionally determined

The abundance of sarcomere mutant and wild-type transcripts were equivalent for all 11 missense mutations examined. A previous study reported variability in the fraction of mutant mRNA for 5 *MYH7* variants,³⁹ but was limited by use of skeletal muscle biopsies, analysis of benign variants, and less sensitive methods than the primer extension technique. While it is possible that differences could be due to specific mutations analyzed, we think this is a less plausible explanation given that non-PTC containing transcripts are not substrates for NMD, and should be intrinsically stable.

Despite comparable transcript levels, mutant to wild-type protein stoichiometry varied considerably for different missense mutations, consistent with previous reports for several *MYH7* mutant proteins in skeletal and cardiac muscle.^{39, 40} An important distinction from previously published methodologies is the recognition of missed cleavages and post-translational modifications which was critical for accurate absolute and relative quantification of wild-type and mutant peptides by AQUA. For one mutation, MYBPC3 Arg495Gln, the mutant peptide was similarly ~2-fold more abundant than wild-type in 2 samples from unrelated HCM patients, implying that preferential expression or stability of the mutant protein is an inherent property of a particular mutant protein rather than a function of other modifying factors. However, analysis of additional samples harboring an identical mutation will be needed to determine whether any component of phenotypic heterogeneity, characteristic of human cardiomyopathies in general, is related to the ratio of wild-type to mutant proteins. Lack of disparity in relative abundance of wild-type and mutant *MYH7* proteins in 2 transplanted hearts across different myocardial segments suggests that regional variation in mutant protein abundance is unlikely to account for the characteristic asymmetric hypertrophy and associated regional mechanical deficits observed in HCM,⁴¹ at least for the mutations studied.

Given equal mutant and wild-type transcript levels, and presuming that protein synthesis is unlikely affected by single missense mutations, our data support the scenario that mutant and corresponding wild-type proteins differ in their intrinsic stability and/or avidness of binding with other partners within the sarcomere. Efficiency of sarcomere incorporation is higher for certain mutant proteins compared to their wild-type counterparts,⁴² while others have a lower efficiency of incorporation or are not tolerated at higher expression levels.⁴³ The magnitude of a dominant negative effect is a function of the “dose” of mutant protein in experimental assays,⁴⁰ and animal models.^{44, 45} Consistent with this dose-response, RNA silencing in a heterozygous mutant *MYH6* mouse model that results in a 28.5% relative reduction in the mutant transcript leads to a dramatic normalization of the phenotype.⁴⁶ However, incorporation of even a small amount of certain mutant proteins may be sufficient to cause disease if they exert a more potent effect in disrupting sarcomere function.⁴³ Missense mutations can also cause protein misfolding, interfering with sarcomere incorporation or resulting in increased susceptibility to degradation. In this latter case, excess production of mutant protein from a stable transcript could be toxic by overwhelming protein quality control systems. In this context, the correlation of absolute allelic imbalance with younger patient age suggests an additional layer of complexity in the relationship between specific mutations and the severity of clinical phenotypes. Overall, these findings support the idea that allelic balance may influence genotype-phenotype correlations and should be an important consideration in designing experimental systems to accurately model the human disease.

Conclusions

This comprehensive and quantitative analysis of mutant sarcomere gene and protein abundance in samples from HCM patients highlights the genetic complexity and allelic variation in this disease. Heterogeneous expression patterns suggest mutation-specific consequences that cannot readily be predicted solely on the basis of the location or type of mutation. As sarcomere gene mutations underlie the genetic basis for a broad range of genetic cardiomyopathies,³ the findings reported here have important implications for disease mechanisms and development of genotype-guided therapies beyond HCM.

Supplementary Material

Refer to Web version on PubMed Central for supplementary material.

Acknowledgments

Funding Sources: NIH R01HL093338 (SMD), R01HL105826 and K02HL114749 (SS), private donation (Help4hcm.com)

References

1. Maron BJ, Maron MS. Hypertrophic cardiomyopathy. *Lancet*. 2013; 381:242–255. [PubMed: 22874472]
2. Maron BJ, Maron MS, Semsarian C. Genetics of hypertrophic cardiomyopathy after 20 years: Clinical perspectives. *J Am Coll Cardiol*. 2012; 60:705–715. [PubMed: 22796258]

3. Watkins H, Ashrafian H, Redwood C. Inherited cardiomyopathies. *N Engl J Med*. 2011; 364:1643–1656. [PubMed: 21524215]
4. Andersen PS, Havndrup O, Bundgaard H, Larsen LA, Vuust J, Pedersen AK, et al. Genetic and phenotypic characterization of mutations in myosin-binding protein c (mybpc3) in 81 families with familial hypertrophic cardiomyopathy: Total or partial haploinsufficiency. *Eur J Hum Genet*. 2004; 12:673–677. [PubMed: 15114369]
5. Carrier L, Schlossarek S, Willis MS, Eschenhagen T. The ubiquitin-proteasome system and nonsense-mediated mrna decay in hypertrophic cardiomyopathy. *Cardiovasc Res*. 2010; 85:330–338. [PubMed: 19617224]
6. Linde L, Kerem B. Introducing sense into nonsense in treatments of human genetic diseases. *Trends Genet*. 2008; 24:552–563. [PubMed: 18937996]
7. Vignier N, Schlossarek S, Fraysse B, Mearini G, Kramer E, Pointu H, et al. Nonsense-mediated mrna decay and ubiquitin-proteasome system regulate cardiac myosin-binding protein c mutant levels in cardiomyopathic mice. *Circ Res*. 2009; 105:239–248. [PubMed: 19590044]
8. Marston S, Copeland O, Jacques A, Livesey K, Tsang V, McKenna WJ, et al. Evidence from human myectomy samples that mybpc3 mutations cause hypertrophic cardiomyopathy through haploinsufficiency. *Circ Res*. 2009; 105:219–222. [PubMed: 19574547]
9. van Dijk SJ, Dooijes D, dos Remedios C, Michels M, Lamers JM, Winegrad S, et al. Cardiac myosin-binding protein c mutations and hypertrophic cardiomyopathy: Haploinsufficiency, deranged phosphorylation, and cardiomyocyte dysfunction. *Circulation*. 2009; 119:1473–1483. [PubMed: 19273718]
10. Crehalet H, Millat G, Albuissou J, Bonnet V, Rouvet I, Rousson R, et al. Combined use of in silico and in vitro splicing assays for interpretation of genomic variants of unknown significance in cardiomyopathies and channelopathies. *Cardiogenetics*. 2012; 2:26–31.
11. Bonne G, Carrier L, Bercovici J, Cruaud C, Richard P, Hainque B, et al. Cardiac myosin binding protein-c gene splice acceptor site mutation is associated with familial hypertrophic cardiomyopathy. *Nat Genet*. 1995; 11:438–440. [PubMed: 7493026]
12. Wappenschmidt B, Becker AA, Hauke J, Weber U, Engert S, Kohler J, et al. Analysis of 30 putative brca1 splicing mutations in hereditary breast and ovarian cancer families identifies exonic splice site mutations that escape in silico prediction. *PloS one*. 2012; 7:e50800. [PubMed: 23239986]
13. Marston S, Copeland O, Gehmlich K, Schlossarek S, Carrier L. How do mybpc3 mutations cause hypertrophic cardiomyopathy? *J Muscle Res Cell Motil*. 2012; 33:75–80. [PubMed: 22057632]
14. Sequeira V, Wijnker PJ, Nijenkamp LL, Kuster DW, Najafi A, Witjas-Paalberends ER, et al. Perturbed length-dependent activation in human hypertrophic cardiomyopathy with missense sarcomeric gene mutations. *Circ Res*. 2013; 112:1491–1505. [PubMed: 23508784]
15. Theis JL, Bos JM, Theis JD, Miller DV, Dearani JA, Schaff HV, et al. Expression patterns of cardiac myofilament proteins: Genomic and protein analysis of surgical myectomy tissue from patients with obstructive hypertrophic cardiomyopathy. *Circ Heart Fail*. 2009; 2:325–333. [PubMed: 19808356]
16. Palacios IM. Nonsense-mediated mrna decay: From mechanistic insights to impacts on human health. *Brief Funct Genomics*. 2013; 12:25–36. [PubMed: 23148322]
17. Maquat LE. Nonsense-mediated mrna decay: Splicing, translation and mrnp dynamics. *Nat Rev Mol Cell Biol*. 2004; 5:89–99. [PubMed: 15040442]
18. Neu-Yilik G, Amthor B, Gehring NH, Bahri S, Paidassi H, Hentze MW, et al. Mechanism of escape from nonsense-mediated mrna decay of human beta-globin transcripts with nonsense mutations in the first exon. *RNA*. 2011; 17:843–854. [PubMed: 21389146]
19. Stump MR, Gong Q, Packer JD, Zhou Z. Early lqt2 nonsense mutation generates n-terminally truncated herg channels with altered gating properties by the reinitiation of translation. *J Mol Cell Cardiol*. 2012; 53:725–733. [PubMed: 22964610]
20. Inoue K, Khajavi M, Ohyama T, Hirabayashi S, Wilson J, Reggin JD, et al. Molecular mechanism for distinct neurological phenotypes conveyed by allelic truncating mutations. *Nat Genet*. 2004; 36:361–369. [PubMed: 15004559]

21. Hall GW, Thein S. Nonsense codon mutations in the terminal exon of the beta-globin gene are not associated with a reduction in beta-mrna accumulation: A mechanism for the phenotype of dominant beta-thalassemia. *Blood*. 1994; 83:2031–2037. [PubMed: 8161774]
22. Usuki F, Yamashita A, Higuchi I, Ohnishi T, Shiraishi T, Osame M, et al. Inhibition of nonsense-mediated mrna decay rescues the phenotype in ullrich's disease. *Ann Neurol*. 2004; 55:740–744. [PubMed: 15122717]
23. Gong Q, Stump MR, Zhou Z. Inhibition of nonsense-mediated mrna decay by antisense morpholino oligonucleotides restores functional expression of herg nonsense and frameshift mutations in long-qt syndrome. *J Mol Cell Cardiol*. 2011; 50:223–229. [PubMed: 21035456]
24. Kerr TP, Sewry CA, Robb SA, Roberts RG. Long mutant dystrophins and variable phenotypes: Evasion of nonsense-mediated decay? *Hum Genet*. 2001; 109:402–407. [PubMed: 11702221]
25. Carrier L, Knoll R, Vignier N, Keller DI, Bausero P, Prudhon B, et al. Asymmetric septal hypertrophy in heterozygous cmybp-c null mice. *Cardiovasc Res*. 2004; 63:293–304. [PubMed: 15249187]
26. McConnell BK, Jones KA, Fatkin D, Arroyo LH, Lee RT, Aristizabal O, et al. Dilated cardiomyopathy in homozygous myosin-binding protein-c mutant mice. *J Clin Invest*. 1999; 104:1235–1244. [PubMed: 10545522]
27. Xin B, Puffenberger E, Tumbush J, Bockoven JR, Wang H. Homozygosity for a novel splice site mutation in the cardiac myosin-binding protein c gene causes severe neonatal hypertrophic cardiomyopathy. *Am J Med Genet A*. 2007; 143A:2662–2667. [PubMed: 17937428]
28. van Dijk SJ, Paalberends ER, Najafi A, Michels M, Sadayappan S, Carrier L, et al. Contractile dysfunction irrespective of the mutant protein in human hypertrophic cardiomyopathy with normal systolic function. *Circ Heart Fail*. 2012; 5:36–46. [PubMed: 22178992]
29. McConnell BK, Fatkin D, Semsarian C, Jones KA, Georgakopoulos D, Maguire CT, et al. Comparison of two murine models of familial hypertrophic cardiomyopathy. *Circ Res*. 2001; 88:383–389. [PubMed: 11230104]
30. Sarikas A, Carrier L, Schenke C, Doll D, Flavigny J, Lindenberg KS, et al. Impairment of the ubiquitin-proteasome system by truncated cardiac myosin binding protein c mutants. *Cardiovasc Res*. 2005; 66:33–44. [PubMed: 15769446]
31. Schlossarek S, Schuermann F, Geertz B, Mearini G, Eschenhagen T, Carrier L. Adrenergic stress reveals septal hypertrophy and proteasome impairment in heterozygous mybpc3-targeted knock-in mice. *J Muscle Res Cell Motil*. 2012; 33:5–15. [PubMed: 22076249]
32. Predmore JM, Wang P, Davis F, Bartolone S, Westfall MV, Dyke DB, et al. Ubiquitin proteasome dysfunction in human hypertrophic and dilated cardiomyopathies. *Circulation*. 2010; 121:997–1004. [PubMed: 20159828]
33. Flavigny J, Souchet M, Sebillon P, Berrebi-Bertrand I, Hainque B, Mallet A, et al. CooH-terminal truncated cardiac myosin-binding protein c mutants resulting from familial hypertrophic cardiomyopathy mutations exhibit altered expression and/or incorporation in fetal rat cardiomyocytes. *J Mol Biol*. 1999; 294:443–456. [PubMed: 10610770]
34. Yang Q, Sanbe A, Osinska H, Hewett TE, Klevitsky R, Robbins J. A mouse model of myosin binding protein c human familial hypertrophic cardiomyopathy. *J Clin Invest*. 1998; 102:1292–1300. [PubMed: 9769321]
35. Razzaque MA, Gupta M, Osinska H, Gulick J, Blaxall BC, Robbins J. An endogenously produced fragment of cardiac myosin-binding protein c is pathogenic and can lead to heart failure. *Circ Res*. 2013; 113:553–561. [PubMed: 23852539]
36. Cattin ME, Bertrand AT, Schlossarek S, Le Bihan MC, Skov Jensen S, Neuber C, et al. Heterozygous lmnadlk32 mice develop dilated cardiomyopathy through a combined pathomechanism of haploinsufficiency and peptide toxicity. *Hum Mol Genet*. 2013; 22:3152–3164. [PubMed: 23575224]
37. Michele DE, Albayya F, Metzger JM. Thin filament protein dynamics in fully differentiated adult cardiac myocytes: Toward a model of sarcomere maintenance. *J Cell Biol*. 1999; 145:1483–1495. [PubMed: 10385527]
38. Robbins J. Remodeling the cardiac sarcomere using transgenesis. *Annu Rev Physiol*. 2000; 62:261–287. [PubMed: 10845092]

39. Tripathi S, Schultz I, Becker E, Montag J, Borchert B, Francino A, et al. Unequal allelic expression of wild-type and mutated beta-myosin in familial hypertrophic cardiomyopathy. *Basic Res Cardiol.* 2011; 106:1041–1055. [PubMed: 21769673]
40. Di Domenico M, Casadonte R, Ricci P, Santini M, Frati G, Rizzo A, et al. Cardiac and skeletal muscle expression of mutant beta-myosin heavy chains, degree of functional impairment and phenotypic heterogeneity in hypertrophic cardiomyopathy. *J Cell Physiol.* 2012; 227:3471–3476. [PubMed: 22213221]
41. Yang H, Carasso S, Woo A, Jamorski M, Nikonova A, Wigle ED, et al. Hypertrophy pattern and regional myocardial mechanics are related in septal and apical hypertrophic cardiomyopathy. *J Am Soc Echocardiogr.* 2010; 23:1081–1089. [PubMed: 20650608]
42. Davis J, Wen H, Edwards T, Metzger JM. Allele and species dependent contractile defects by restrictive and hypertrophic cardiomyopathy-linked troponin i mutants. *J Mol Cell Cardiol.* 2008; 44:891–904. [PubMed: 18423659]
43. Tardiff JC, Factor SM, Tompkins BD, Hewett TE, Palmer BM, Moore RL, et al. A truncated cardiac troponin t molecule in transgenic mice suggests multiple cellular mechanisms for familial hypertrophic cardiomyopathy. *J Clin Invest.* 1998; 101:2800–2811. [PubMed: 9637714]
44. James J, Zhang Y, Osinska H, Sanbe A, Klevitsky R, Hewett TE, et al. Transgenic modeling of a cardiac troponin i mutation linked to familial hypertrophic cardiomyopathy. *Circ Res.* 2000; 87:805–811. [PubMed: 11055985]
45. Ahmad F, Banerjee SK, Lage ML, Huang XN, Smith SH, Saba S, et al. The role of cardiac troponin t quantity and function in cardiac development and dilated cardiomyopathy. *PLoS one.* 2008; 3:e2642. [PubMed: 18612386]
46. Jiang J, Wakimoto H, Seidman JG, Seidman CE. Allele-specific silencing of mutant myh6 transcripts in mice suppresses hypertrophic cardiomyopathy. *Science.* 2013; 342:111–114. [PubMed: 24092743]

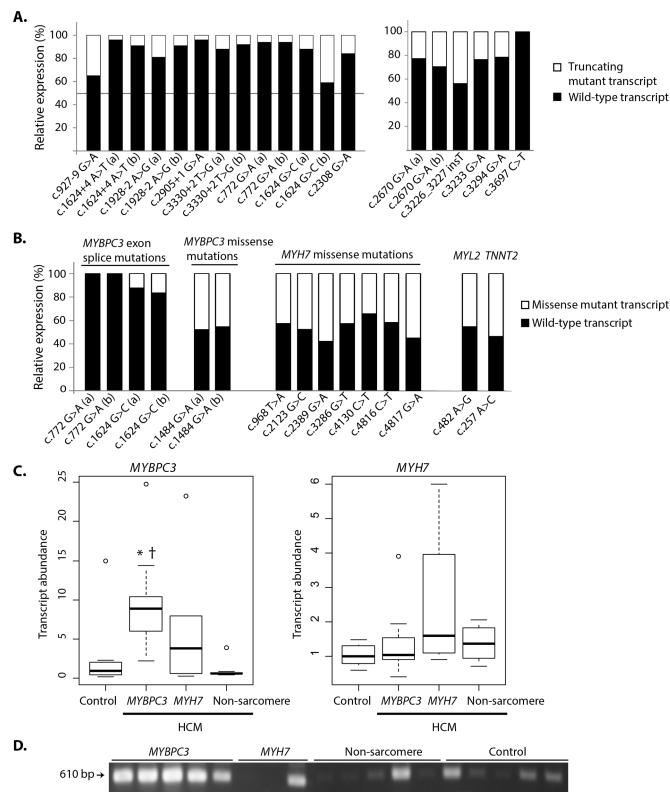


Figure 1.

Sarcomere gene expression in human HCM samples. **A.** (Left) Allele-specific expression from wild-type and *MYBPC3* splice-error PTC-containing transcripts quantified by RT-qPCR with custom designed primers (Supplementary Table 5). (Right) Allele-specific expression from wild-type and *MYBPC3* PTC-containing transcripts (without splice errors) quantified by custom-designed single base extension reactions. These mutations are either single nucleotide substitutions that encode for a termination codon, or an insertion that causes a frameshift. **B.** Quantification of wild-type and single nucleotide substitution mutant sarcomere gene transcripts without PTCs by custom-designed single base extension reactions. For the *MYBPC3* exon splice site mutations, the mutant fraction is the proportion of detectable missense transcript. The remainder of the samples contain true missense mutations. In instances where 2 samples carried the same mutation, these are designated as (a) and (b) respectively in this figure, and maintained throughout the manuscript. **C.** Total *MYBPC3* transcript abundance (left panel) and total *MYH7* transcript abundance (right panel) in carriers of *MYBPC3* (n=18) or *MYH7* (n=6) mutations, compared to HCM samples in which no sarcomere mutation (n=7) was identified and control (non-HCM donor, n=7) hearts. *P=0.02 vs. control hearts, †P=0.003 vs. non-sarcomere HCM. **D.** RT-PCR analysis showing uniformly increased intensity of amplified *MYBPC3* sequence in samples containing *MYBPC3* mutations compared to the other 3 groups.

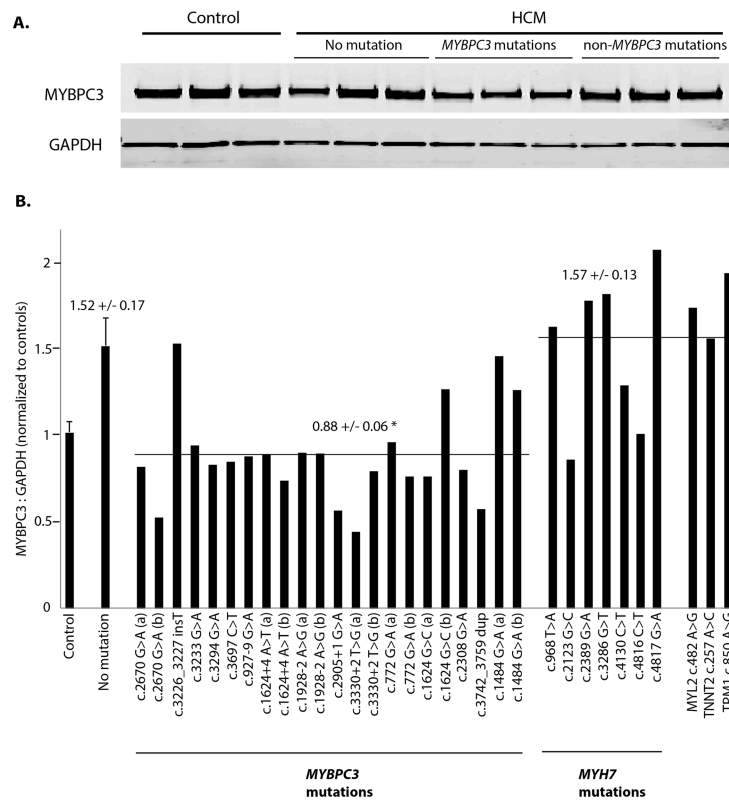


Figure 2. MYBPC3 protein level. **A.** Representative western blot and **B.** Graph summary of densitometric analysis for MYBPC3 protein normalized to GAPDH and expressed as a % of the average of controls run on each gel. Results are shown for control, non-failing hearts (N=10), and HCM hearts without sarcomere mutations (N=14), with MYBPC3 mutations (N=22), and with sarcomere mutations other than MYBPC3 (N=10). *P<0.001 for HCM with MYBPC3 mutations vs HCM with or without other sarcomere mutations, †P<0.05 for HCM without sarcomere mutations vs controls and for HCM with non-MYBPC3 sarcomere mutations vs controls.

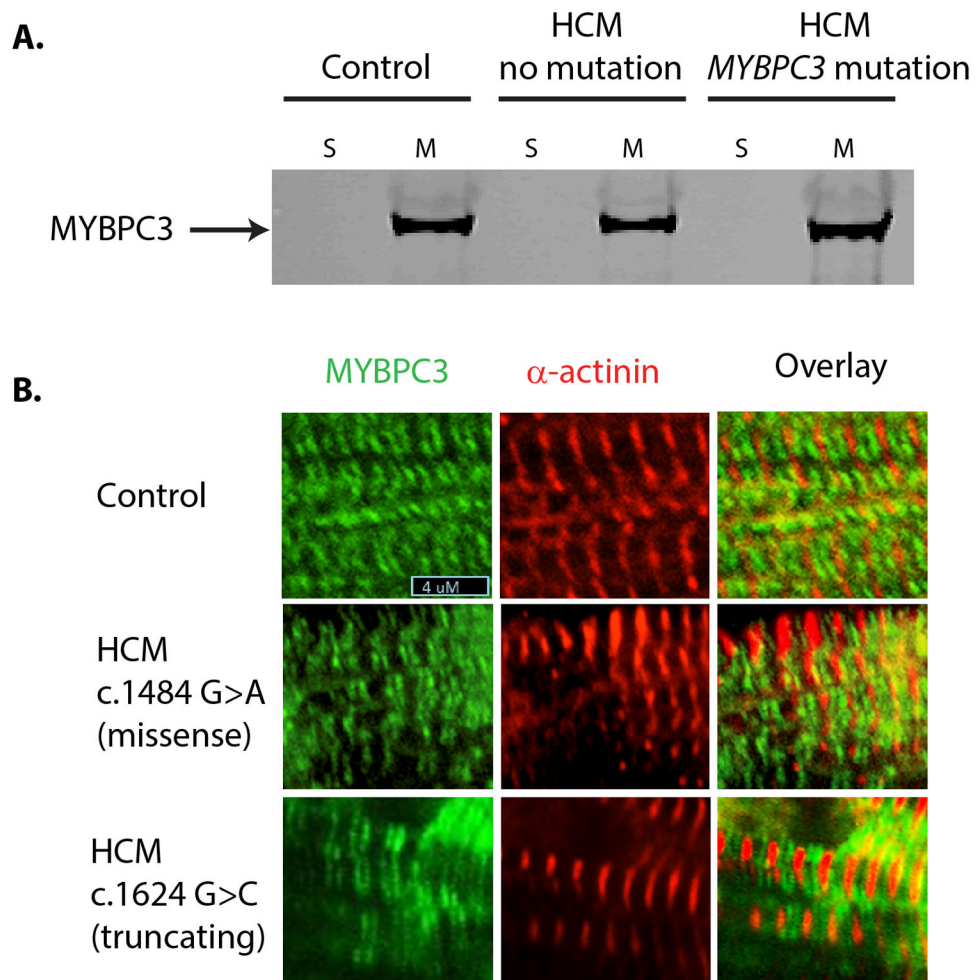


Figure 3. MYBPC3 localization. **A.** Representative western blot for MYBPC3 of samples containing various MYBPC3 mutations shows that all MYBPC3 protein is detected in the myofilament fraction, and none in the supernatant. **B.** Representative immunofluorescent images of formalin-fixed heart tissue from human hearts, reacted with antibodies to MYBPC3 (green) and α -actinin (red) showing correct localization of MYBPC3 to the A-b and of the sarcomere in a doublet pattern. This localization pattern was observed in all truncating and missense mutant samples examined.

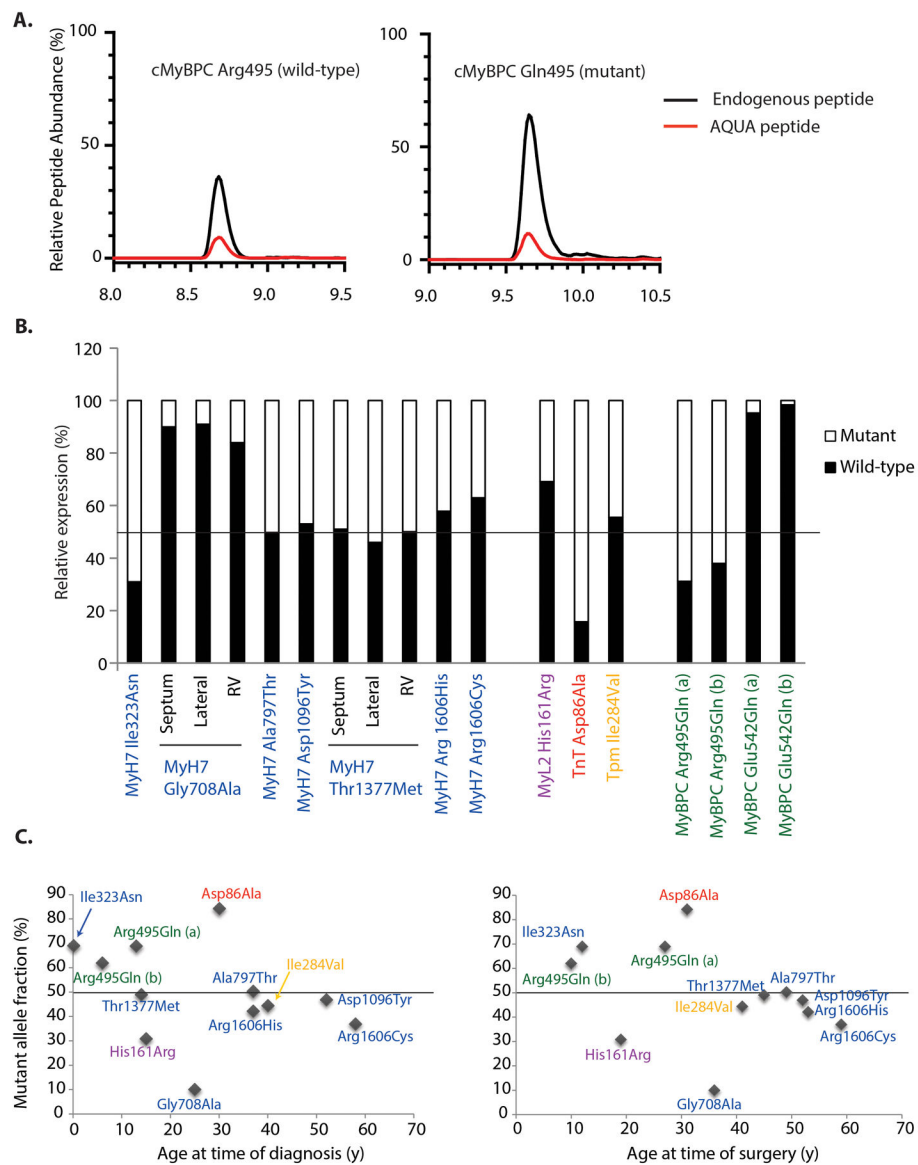


Figure 4. Stoichiometry of wild-type and mutant sarcomere protein in human HCM determined by absolute quantification of abundance (AQUA). **(A)** Representative chromatogram from HCM sample MYBPC3 Arg495Gln (a) showing peptide abundance of wild-type and mutant peptides relative to their corresponding AQUA peptides. **(B)** Graph summary of relative peptide abundance of wild-type and mutant peptides from individual samples. The abundance of each peptide(s) (fmol) was calculated, summed in cases of missed cleavages or post-translational modifications (Supplementary Table 4), and expressed as a relative percentage of the total (abundance of wild-type + mutant peptides for each sample). Three regions (septum, LV lateral wall, and right ventricle) were analyzed in 2 samples with MYH7 mutations obtained from explanted hearts at the time of transplantation. For both B and C, color coding is used to designate genes harboring mutations: MYH7 (blue), MYBPC3 (green), TNNT2 (red), TPM1 (yellow), MYL2 (purple). **(C)** Relationship of

patient age at time of surgery (left panel) and age at time of diagnosis of HCM (right panel) to mutant allele fraction. There was a significantly greater degree of allelic imbalance (in either direction) in patients who had surgery ≤ 40 y/o, compared to those > 40 y/o ($P < 0.01$) and in patients who were diagnosed ≤ 30 y/o, compared to those diagnosed > 30 y/o ($P < 0.05$).

Table 1

Patient Demographics and Echocardiographic Measurements

	Age (y)	% male	Septal thickness (mm)	EF (%)	L VOT gradient (mmHg)
Controls (n=10)	52 ± 5	40	11.8 ± 0.7	60 ± 2	-
HCM patients					
No sarcomere mutation (n=14)	51 ± 3	64	19.9 ± 1.2*	70 ± 2	79 ± 16
Non- <i>MYBPC3</i> mutations (n=10)	40 ± 5	50	19.3 ± 0.8*	72 ± 3*	78 ± 13
<i>MYBPC3</i> mutations (n=22)	40 ± 3	50	24.2 ± 1.7*	70 ± 3*	78 ± 10

EF = ejection fraction, L VOT = Left ventricular outflow tract. Gradient measured at rest in myectomy patients only.

* P<0.05 vs controls.